JOURNAL OF CATALYSIS 148, 417–426 (1994)

CO Chemisorption on Cobalt Clusters: Choosing Clusters for Theoretical Analysis of Surface/Adsorbate Interactions

M. C. Zonnevylle,* J. J. C. Geerlings,* and R. A. van Santen†

*Koninklijke/Shell-Laboratorium Amsterdam (Shell Research B.V.), Badhuisweg 3, 1031 CM Amsterdam, The Netherlands; and †Laboratory of Inorganic Chemistry and Catalysis, Eindhoven University of Technology, P.O. Box 513, 5600 MB Eindhoven, The Netherlands

Received February 1, 1993; revised February 2, 1994

Local density calculations of CO bound to various cobalt clusters are described with the aim of determining the chemistry of the cluster as accurately as possible, and subsequently translating this into the chemistry of the metal surface. Highlighted is the importance of using an invariant cluster to compare binding site characteristics. Variations in the binding energy of CO to the clusters can be most readily ascribed to variations in cluster size and shape. Differences in energy are due primarily to the "cluster chemistry," i.e., different responses of the cluster electrons to the adsorbate, rather than differences in the cluster–adsorbate interaction as such. An important factor is the coordination sphere of the cluster atoms; at least one should have a bulklike coordination, others must have a lower coordination to simulate the surface. Thus it is important to construct a single cluster to study adsorbate–adsorbent interactions, in which the cluster atom coordination spheres are taken into account. © 1994 Academic Press, Inc.

I. INTRODUCTION

The investigation of the binding of CO to metal surfaces has become a perennial favorite of both experimental and theoretical surface scientists. This is not without reason. Developing a detailed understanding of the processes of CO adsorption and dissociation is of paramount importance in the microscopic investigation of numerous catalytic reactions. One of the more important is the Fischer–Tropsch reaction, which entails the conversion of synthesis gas, a mixture of CO and H_2, to saturated and unsaturated hydrocarbon or oxygenate products over suitable metal catalyst surfaces. In addition, the CO molecule considered purely as an adsorbate on a surface serves as a ready tie between the world of surface science and that of organometallic chemistry, in which CO as a ligand plays an important role. Lastly, the analysis of the binding of CO to a metallic surface, or to a metal atom in a molecular complex, has been singled out as the classic example of a synergistic interaction between bonding and back-bonding components. The donation of the occupied CO 5σ orbital into empty metal d levels and their back-donation into the unoccupied degenerate CO $2\pi^*$ levels is called the Blyholder interaction by the surface scientist (1); the same descriptive model is referred to as the Dewar–Chatt–Duncanson model by the organometallic chemist. However, this is an oversimplification of adsorbate–adsorbent interaction; completely ignored is the Pauli repulsion, which is essential to understanding adsorbate coordination behaviour. There is a need to integrate the Blyholder model with Hoffmann's bonding–antibonding fragment orbital analysis (2), specifically in the case of a metallic adsorbent (hereafter termed the substrate) with an essentially constant energy Fermi level.

As part of an ongoing investigation of the Fischer–Tropsch reactivity of various cobalt single crystal surface (3), this paper will focus on discussing the binding characteristics of CO to cobalt cluster models. Cluster methods have well-known advantages and disadvantages; Koutecky and Fantucci have written an excellent review on the subject (4). The feasibility of using cluster models will depend to a great extent on the degree to which the interaction can be classified as "local." Much of the success of the approximation lies in a judicious choice of both the problem to address and the specific cluster geometry. Thus, one of the most crucial steps in performing computer modeling studies on the catalytic behaviour of metal surfaces comes in choosing the proper model to represent the metal surface. Accurate quantum chemical computational methods are usually restricted in the maximum number of atoms per model. The Amsterdam local density approximation (LDA) code (5) we have employed is limited to molecular systems; thus metallic surfaces must be represented by small metal clusters. The specific choice of cluster is dictated by several factors, most importantly that the cluster should be:

(1) as highly symmetric as possible;
(2) sufficiently large to exhibit "metallic" characteristics;
(3) sufficiently large to give reasonably low adsorbate-to-substrate atom ratios;
(4) sufficiently small to be computationally reasonable.

0021-9517/94 $6.00

Usually, clusters are built by choosing a number of metal atoms in the surface layer and optionally several in the second layer which model the bulk. However, the typical result is that the coordination number of the model surface atom(s) to which adsorbate is bound is higher than that of the atoms which are meant to model the bulk. This is in conflict with the real situation, in which surface atoms are undercoordinated in comparison to the bulk.

The difficulty will arise, in particular, when comparing the binding energies of one adsorbate to different model clusters, for example when comparing the adsorption of carbon monoxide at atop, bridging, and hollow sites on Co(0001). The model surface atoms in this case are not only overcoordinated in comparison to their model bulk atom neighbours, but also the degree of overcoordination can vary from cluster to cluster. The problem will be further magnified if no geometry optimisation is performed on the adsorbate–cluster bond, as this should somewhat compensate for the artificial influence of varying the coordination spheres of the model surface atoms.

One possible solution is to construct special clusters in which the atoms representing the surface and adsorption site have a low coordination number, and one (or more) other cluster atom has the coordination sphere of the bulk (12 for *hcp* Co). In addition, the cluster can be chosen so that the model surface atoms all have the same coordination number, allowing a direct comparison between different coordination sites on the cluster. The hypothesis that this will alleviate the inconsistency in binding energies and other calculated parameters has not previously been tested, as the required clusters are large. Open surfaces and edge or step sites can be modeled with cluster sizes attainable by current ab initio methods. To test this hypothesis, we have selected the smallest *hcp* cluster which fulfils the above requirements, i.e., a 13-atom cluster, and the chemical "test case" of CO adsorption and C–O bond weakening on cobalt cluster surfaces.

II. METHOD

The Hartree–Fock–Slater–LCAO discrete variational method (HFS–LCAO) is one of a number of possible methods used to analyse chemisorptive interactions by means of metal cluster models. Other work on HFS–LCAO clusters (6) provides evidence that the method can be used to properly model trends, although the absolute values of calculated properties may be incorrect. The present study uses the Amsterdam local density code, which includes implementation of the Ziegler transition state method (7). The Vosko–Wilk–Nusair local spin density functional was used, with Stoll, Becke, and Perdew corrections in place. The Slater-type orbital (STO) basis sets are listed in Table 1 (8). For Co, the basis consists of single-zeta core functions for the frozen core up to 3*p*, triple-zeta 3*d*, triple-zeta 4*s*, and single-zeta 4*p*. Frozen cores were also adopted for C and O, with double-zeta 2*s* and 2*p*, and single-zeta 3*d*. Polarization fit functions have been added for all atoms.

TABLE 1

Exponential Coefficients for Basis Functions

Co	C	O
1*s*[a] 14.10	1*s*[a] 5.40	1*s*[a] 7.36
2*s*[a] 11.65	2*s* 1.24	2*s* 1.70
3*s*[a] 4.85	2*s* 1.98	2*s* 2.82
2*p*[a] 10.74	2*p* 0.96	2*p* 1.30
3*p*[a] 4.18	2*p* 2.20	2*p* 3.06
3*d* 1.50	3*d* 2.50	3*d* 2.00
3*d* 3.25		
3*d* 6.70		
4*s* 0.48		
4*s* 1.40		
4*s* 2.40		
4*p* 1.43		

[a] Additional functions added for core orthogonalization.

II. RESULTS AND DISCUSSION

A. Bare Clusters

Atop, bridging, and threefold hollow sites were considered for CO adsorption onto the close-packed Co(0001) surface. For each CO site, two different cobalt clusters built in the "traditional" manner were chosen. The six models are t1, b1, h1, t2, b2, and h2, shown in Fig. 1. In each case, Co(1) is always bound to CO, and Co(2) is its nearest neighbour, preferentially in the surface plane. The pairs of clusters t1 and t2, and b1 and b2 differ by the addition of three cobalt atoms in the second layer. The h1 and h2 pair not only differ in size, but also represent the two different threefold hollow sites available on all close-packed surfaces. For h1, a second layer metal atom lies directly below the CO site (the *hcp* site), whereas no second layer atom lies below the CO site for h2 (the *fcc* site). In addition to these 6 models, the above-described 13-atom *hcp* cluster was contructed, suitable for all three sites. The 12 equivalent surface atoms (Co(1)) have a low coordination number (5); the central atom (Co(2)) has the bulk cobalt coordination number of (12). Top, bridging, and hollow CO coordination models, respectively t3, b3, and h3, are also shown in Fig. 1. Note that these clusters do not represent the (0001) surface. The geometry of all the cobalt clusters was taken directly from bulk metal values; no geometric optimization was performed on the bare clusters. This would be extremely demanding with respect to CPU time. In addition, we believe that the

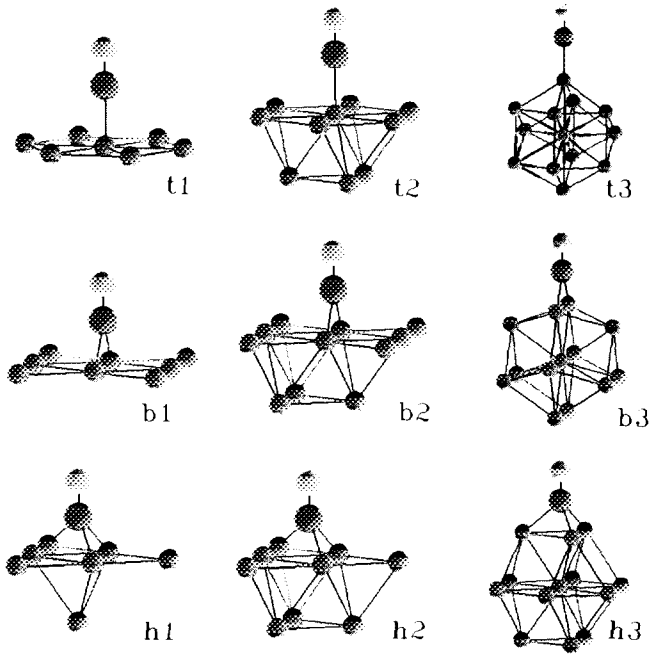

FIG. 1. Models used in the CO–cobalt cluster calculations. t1, t2, and t3 represent atop sites, b1, b2, and b3 represent bridging sites, and h1, h2, and h3 represent hollow sites. Carbon atoms are the darkest balls, oxygen atoms the lightest. CO is always bound at the carbon end, and standing perpendicular to the surface.

general trends of surface/adsorbate interactions covered in this study should most be greatly affected.

Before considering the binding of CO to these clusters, certain characteristics which make clusters more or less suitable for the modeling of surfaces should be emphasized. Considerations specific to the HFS–LCAO treatment of the bare h2 cluster have been discussed by us in a previous paper (9). For example, the localization of charge on any one metal center in h2 was found to be very low, maximally 0.020 *e*- excess on Co(1). It was previously noted that this result may have been fortuitous. Indeed, this particular cluster is found to exhibit an unusually low degree of charge localization. Table 2 lists the net atomic charges found for the bare clusters. The greatest degree of charge localization is, in fact, found on the central atom of the 13-atom cluster, with net charge +0.2660. Thus the surface atoms of this cluster are slightly negatively charged relative to the bulk, just as is expected for metals in which the Fermi energy ε_f falls above the middle of the *d* band. The *d* bands of the surface atoms are narrower (less disperse) than those of the bulk because the surface atom coordination number is lower.

Also of importance is the average electronic configuration in the clusters. These values are listed in Table 3 and compared to experimental and spin-polarized local spin density atomic results. The 3*d* occupation varies little throughout the cluster series, between 7.87 and 7.91 *e*-.

TABLE 2

Atomic Charges of Bare Cobalt Clusters

Model	Co(1)	Co(2)	Co(3)
t1	+0.008	−0.001	—
t2	−0.0118	+0.021	−0.003
t3	−0.022	+0.266	—
b1	−0.031	−0.024	—
b2	−0.049	−0.031	+0.021
b3	−0.022	+0.266	—
h1	−0.054	−0.010	+0.191
h2	−0.020	+0.002	+0.017
h3	−0.022	+0.266	—

Note. Co(1) will be bound to CO, Co(2) is its nearest neighbour, preferentially in the surface plane, and Co(3) is its next-nearest neighbour.

These values lie very close to the atomic results. In addition, the 3*d* occupation is fairly invariant to the coordination sphere; the average difference between Co(1) and Co(2) is, for example, only −0.09 *e*-. Apparently, there is a sufficient number of *d* states in the cluster to form a "band." More variation is observed in the average 4*s* and 4*p* results, which is to be expected from the comparatively few occupied *s* and *p* states (the delocalization effect). This will clearly have consequences in the Pauli repulsion term in particular. For these states, the coordination geometry has a clear influence on the occupation; the higher the coordination number, the lower the 4*s* filling. The Co(1) 4*s* is filled by 0.25 *e*- less than Co(2), whereas Co(1) 4*p* is filled by 0.35 *e*- more than Co(2), on the average. Most striking is that the 4*s* occupation of the central atom Co(2) of the 13-cobalt cluster is nearly zero. This, however, can be rationalized by considering that for the fully bonding *s* orbital combination of an oligomer, the maximal

TABLE 3

Average Electronic Configuration of Co Valence Levels in Bare Clusters

Model	4*s*	4*p*	3*d*
t1	0.82	0.27	7.91
t2	0.72	0.41	7.87
t3	0.68	0.44	7.88
b1	0.86	0.27	7.81
b2	0.75	0.36	7.89
b3	0.68	0.44	7.88
h1	0.52	0.28	7.88
h2	0.77	0.38	7.85
h3	0.68	0.44	7.88
Atomic exp.	2	—	7
LSD calc. (12)	1.1	—	7.9

orbital density will reside on the "end" atoms. This effect will be particularly strong in the spherical 13-atom cluster. Additionally, by symmetry, the Co(2) s orbital can participate only in this orbital and its empty antibonding counterpart. A more reliable manner in which to probe the extent to which the clusters may properly model a surface is to examine the manner in which the states are spread in energy, rather than to compare only the total charges. In each case, the total density of states (DOS) exhibits a dense band of spatically delocalized d states overlapping the higher energy, and more diffuse s–p region. The energetic gap between the higher occupied molecular orbital (HOMO), which may be considered as the "cluster Fermi energy," ε_f, and the lowest unoccupied molecular orbital (LUMO) is very small and lies in the upper part of the d band.

Self-consistent convergence to the ground electronic state is difficult to achieve, indicating that several closely spaced excited states exist near the ground state. All of these characteristics resemble those of a real surface. It is likely that the local densities of states (LDOS) at the surface atoms resemble those of true surface d levels. However, because of the sparse nature of the s and p levels, their LDOS will converge much more slowly. Whether this will be problematic in adsorbate–substrate modeling is dependent on the relative strengths of the metal s–s interaction and the metal s–adsorbate interaction. A measure of the change in the relative importance of the s-character in different clusters is the difference in energy between ε_f and the HOMO of dominantly s-character. The absence of a large variation would indicate that cluster excitation effects to reduce Pauli repulsion are comparable between the clusters. However, because of the symmetry of the clusters, the metal s-character is spread rather uniformly over the states of predominantly d-character, yielding no specific state of primarily s-character. The cohesive energies of the clusters compare well with those of bulk cobalt. The computed cohesive energies per atom range from -4.711 eV for t2 to -5.554 eV for the 13-atom cluster. The experimental value per bulk cobalt atom is -4.40 eV (10). The computed cohesive energy is particularly sensitive to the choice of density functional and inclusion of nonlocal correction terms; using the $X-\alpha$ functional, and neglecting correction terms, the computed values range from -5.246 to -6.305 eV. Considering the importance of the model atom coordination numbers, a more valid comparison may be made by normalizing the cohesive energy to the total coordination number. This gives an average atom–atom bond energy. If the total cohesive energy is divided by the sum of the coordination spheres, the results fall into three well-defined groups. The smallest clusters, i.e., those most coordinatively unsaturated (t1, b1, and h1), have an average bond energy of approximately -1.40 eV. The t2, b2, and h2 clusters all lie close to -1.11 eV and the 13-atom cluster value is -1.00 eV. The experimental bulk value is -0.73 eV. The greater the coordinative unsaturation of the atoms, the more electron localization and the greater the bond strength per metal–metal bond.

B. CO on Clusters

a. Energetic considerations. The molecular levels of CO are well known. Briefly, two orbitals are of primary importance to chemisorption, namely the highest occupied molecular orbital (HOMO) 5σ and the lowest unoccupied molecular orbital (LUMO) $2\pi^*$. The 5σ state is best described as the carbon lone pair orbital, but it is also slightly bonding between C and O. The degenerate $2\pi^*$ pair of orbitals is strongly antibonding between C and O. Relative to the electronic spectrum of cobalt, the 5σ states of free CO fall ~ 1.5 eV below the bottom of the d band, and ~ 5.0 eV below ε_f. The $2\pi^*$ state lies ~ 1.0 eV above the top of the d band and ~ 2.0 eV above ε_f. CO chemisorption onto metal surfaces is often described in terms of the Blyholder mechanism, as a synergism between electron transfer from the 5σ to the metal levels (5σ bonding) and backtransfer from the metal levels into the $2\pi^*$ ($2\pi^*$ backbonding). Note that both effects will reduce the strength of the C–O bond, thus promoting dissociation.

The Blyholder model, however, is an oversimplification. Because the 5σ state is fully occupied, we must expect Pauli repulsion with occupied surface electronic states. This effect has also been described by Bagus *et al.* (11) and by Post and Baerends (12). The effect is reduced if the antibonding levels are pushed above ε_f (13). In addition, simple $2\pi^*$ backbonding with the d-levels should result in a metal–CO antibonding level of predominantly $2\pi^*$ character (as well as a lower energy bonding level of predominantly metal character) which lies at a higher energy than the free CO $2\pi^*$ level. However, inverse photoemission studies of CO adsorbed on Pd (14) and Ag (15) surfaces suggest that the metal–CO $2\pi^*$ antibonding level can be found at a *lower* energy than in the free CO. This is attributed to the interaction with the surface s and p orbitals. Our results are consistent with these experimental studies; for example, the $2\pi^*$ level for atop bound CO drops approximately 1.0 eV in energy. Experimental studies propose that at low coverages (less than 1/3 of a monolayer), CO binds atop on Co(0001) (16), with a binding energy of 128 kJ/mol (1.3 eV) (17). At higher coverages, both bridging and atop sites become populated (16). As yet, neither the C–O nor the C–Co distance is known for this system. So as not to bias the calculations, the C–O distance was initially fixed at that of gas phase CO, 1.130 Å (2.132 a.u.). This value is almost certainly too short for CO adsorbed onto a surface. In addition, one might expect the bond to lengthen as the

coordination number increases. However, since we are interested in relative trends in the first instance, rather than the absolute values of computed parameters, and since we wish to be able to compare the results from the different sites in an unbiased manner, we initially retained this fixed distance. Later in this paper, we shall discuss some geometry-optimized results. The C–Co distance was set to 1.900 Å (3.592 a.u.), a typical distance for organo-cobalt complexes. Thus, the perpendicular C–surface distance is 1.900 Å for the ontop sites, 1.444 Å for the bridged, and 1.256 Å for the hollow sites.

The Ziegler transition state method can be used to split the binding energy (BE) of CO to the various clusters into a repulsive term due to steric interaction E_{st} and an attractive term due to stabilization of the electronic levels (E_{orb}). The energetic breakdowns for the six models are listed in Table 4. E_{orb} can be further decomposed into the contribution per symmetry type. For the binding of CO, the orbital interactions will result from either σ or π levels; these labels have been adopted in Table 4.

For the traditionally constructed models (i.e., all models except t3, b3, and h3), the bridging site is computed to be energetically most favourable. Note that this is in contrast with the experimental result that CO binds atop on Co(0001). Binding energies are generally overestimated with local density methods. If the X-α functional is used rather than the Vosko–Wilk–Nusair local spin density functional, and no corrections are made to the local potential, this overestimation is somewhat worse, varying between 0.1 and 0.3 eV per cluster. In addition, achieving convergence in the electron density requires more iteration cycles.

The 13-atom clusters, however, do reproduce the experiments. The binding energies now show the proper trend: atop > bridging > hollow. In addition, the binding energies are not overestimated as severely. Although we present only a single example, it is our tentative conclusion that overcoordination of model surface atoms severely deteriorates the representativeness of the computed binding energies for metal surfaces, and that proper construction of the clusters may alleviate this problem.

TABLE 4

Binding Energy (eV) of CO to Cobalt Cluster, and Decomposition into steric (E_{st}) and Orbital (E_{orb}) Components

Model	E_{st}	E_{orb}	σE_{orb}	$\pi^* E_{orb}$	BE
t1	5.256	−6.528	5.524	−10.145	−1.271
t2	6.257	−8.259	4.573	−10.128	−2.002
t3	5.497	−7.096	10.463	−14.166	−1.599
b1	9.891	−12.072	2.119	−7.949	−2.181
b2	10.723	−13.354	2.010	−8.175	−2.631
b3	5.208	−6.611	2.768	−5.010	−1.403
h1	12.249	−14.350	0.348	−13.156	−2.102
h2	13.302	−15.717	0.210	−13.778	−2.415
h3					−1.227

Note. E_{orb} is further decomposed by symmetry; the symmetry decomposed values do not include Becke and Perdew correction terms.

The orbital decomposition reveals that the σ contribution to the adsorbate bond is indeed repulsive, as suggested by Bagus *et al.* Because of the directionality of the 5σ orbital, the repulsive interaction is strongest for atop, followed by bridging, then hollow. This simple analysis alone points out the inadequacy of the Blyholder model and the necessity for including Pauli repulsion between full adsorbate states and surface levels. In addition, the $2\pi^*$ level, which is clearly discernible in the projected DOS of the atop case only, drops in energy relative to the gas phase value. Although in contrast with the simple MO picture, this is consistent with experimental results. The $2\pi^*$ state interacts so strongly with the metal levels at other binding sites that no antibonding state can be identified as such.

TABLE 5

Results of Geometry Optimization of C–O and C–Co Distances, on Frozen Clusters

Model	d(C–O) (Å)	d(C–Co) (Å)	d(C–surface) (Å)	BE (eV)
t2	1.086	1.913	1.913	−1.837
b2	1.298	2.049	1.620	−2.517
h2	1.155	2.326	1.819	−2.225

Geometry optimization was performed on three of the nine clusters; t2, b2, and h2. The results presented in Table 5 show the expected increase in the C–Co distance with increasing CO coordination number. A lengthening of the C–O bond from the gas phase value is observed for bridging and hollow sites, but not for the atop mode. Again, we attribute this to overcoordination of the surface model atoms. Unfortunately, performing a geometry optimization on the 13-atom clusters is as yet conputationally prohibitive. Hence the remainder of the discussion will focus on the geometry-constrained systems alone (constant C–O and C–Co distances).

b. Analysis of chemical bonding: Overlap populations and density of states. Semi-empirical methods have long reaped the benefits of analyzing covalent interactions in terms of the Mulliken overlap population (o.p.). The o.p. between two atoms (or between two atomic orbitals) is simply the cross term of their inner product, and, most importantly, scales as the strength of the chemical interaction. The total o.p. can be decomposed into the contribution per symmetry element, and by specific orbital. Because the 5σ and $2\pi^*$ levels carry the dominant

contribution to the chemisorptive bond, the contribution from their respective symmetry group is simply labeled as resulting from these two specific orbitals alone. Figure 2 shows the 5σ and $2\pi^*$ CO–cluster o.p. contributions vs their fractional occupations, and the total CO–cluster o.p. per site. The total o.p. is greatest for the top site, as would be expected from the experimental site preference, as well as from a group orbital analysis (18), less for the bridging sites, and least for the hollow sites. Note that total and decomposed o.p. values depend strictly on the CO site and are essentially independent of cluster size or shape, contrary to the energetic results. The o.p. appears to be a more local property of the CO site, and thus more accurately reflects the experimental site preference. It is not as dependent on secondary effects occurring on the edges of the cluster as is found for the binding energy.

The fractional occupation of the 5σ is nearly site-insensitive, losing between 0.60 and 0.52 e- upon adsorption. Based on the Blyholder model of 5σ donation and $2\pi^*$ backdonation, one would expect equivalent 5σ occupations to produce a more or less constant contribution to the CO–cluster bond. However, the present work shows that the 5σ CO–cluster o.p. contribution is extremely sensitive to site, positive for atop, nearly zero for bridging, and negative for threefold hollow sites. The $2\pi^*$ occupation increases with coordination number, as is often deduced from the decrease of the C–O stretch frequency as measured by, e.g., high resolution electron energy loss spectroscopy (HREELS) with increasing coordination number on a variety of metal surfaces (19). The $2\pi^*$ occupation is most directly dependent on CO site, rather than cluster size. Its contribution to the CO–cluster o.p. does follow the conventional model; the greater the $2\pi^*$ occupation, the larger the contribution to the chemisorptive bond. Thus, with increasing coordination number, the 5σ CO–cluster o.p. decreases, whereas the $2\pi^*$ CO–cluster o.p. increases. The net result is that the atop chemisorptive bond is strongest.

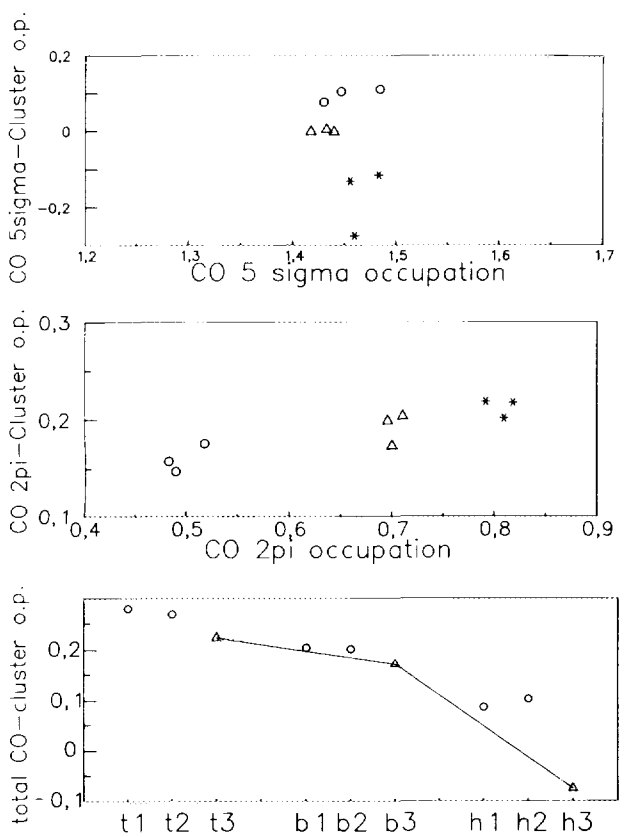

FIG. 2. Decomposition of the CO–cluster overlap population. The top panel shows the contribution to this o.p. from the CO 5σ levels vs the CO 5σ electronic occupation, and the middle panel shows the same for the CO $2\pi^*$ level. Circles represent atop models, triangles bridging models, and stars hollow models. Note that the electronic occupation scales are equivalent. The bottom panel shows the total CO–cluster o.p. for each model; the 13-atom models are highlighted.

In order to understand the factors governing the CO–cluster o.p. it is helpful to consider a combination of analysis techniques:

(1) the projected density of states (PDOS), or local density of states, of the CO molecular orbitals;
(2) their cluster orbital overlap population (COOP) plots, which are analogous to the crystal orbital overlap population curves (20);
(3) the concept of group orbitals.

The COOP plots result from weighting the total DOS according to the contribution, per energy unit, to the strength of a specific bond. The contribution can be positive (bonding) or negative (antibonding). In this case, we are interested in the CO–cluster bond. The PDOS curves are computed using Gaussian broadening functions, but given the individual contributions of the orbitals to the chemisorptive bond may be small, no broadening is applied to the COOP plots.

Figure 3 shows the 5σ PDOS, integrated PDOS, and total DOS of t1, b1, and h2, and Fig. 4 shows their 5σ CO–cluster bond COOP plots. The plots for t2, b2, and h1 are very similar to their respective partner models, and are therefore not shown. The position of the free CO orbitals is indicated with thick bars in the top panel. The 5σ level lies far below ε_f, ~5.0 eV below for free CO and pushed down even further upon adsorption. Although the total filling of the levels is equivalent, as can be seen from the integration value of ~73% at ε_f, the shape of the PDOS varies significantly with site. At the atop site, the 5σ states remain well localized in one peak close to the original energetic position. As the coordination number increases, the 5σ character in this peak decreases from 62 and 33 and 28%. Concurrently, the amount of 5σ mixing into the original 4σ region (near −13 eV) increases from 5% atop to 32% bridging and 42% hollow. One expects

that the 4σ level will be essentially of nonbonding nature in the CO–cluster interaction, as this orbital is primarily localized on the oxygen end of the molecule. However, even the 5σ part of the 4σ region is not of a strongly bonding nature in the CO–cluster interaction. An increase in the 5σ concentration from bridge to hollow in the PDOS is met by a decrease in the CO–cluster o.p. in this region, as seen in the COOP plot. The 4σ–5σ mixing increases with increasing coordination number, due to the stronger repulsion with the metal levels. The mixing will move more of the electron density away from the carbon end, thus lowering the repulsion.

More subtle differences can be discerned in the small 5σ peaks pulled up into the cluster d band. These are best seen in the COOP plots between -8 eV and ε_f. The atop 5σ states are the least antibonding, followed by bridging, then hollow states. The states also generally lie at a higher

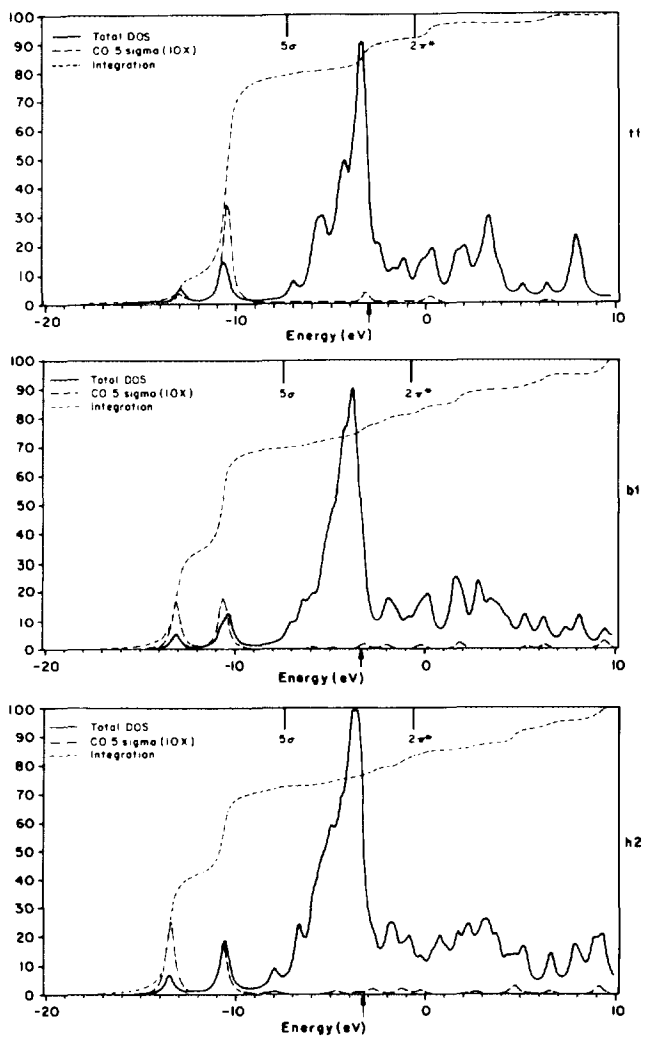

FIG. 3. The total DOS, CO 5σ PDOS, and integration of the CO 5σ levels are depicted for t1 (top panel), b1 (middle panel), and h2 (bottom panel).

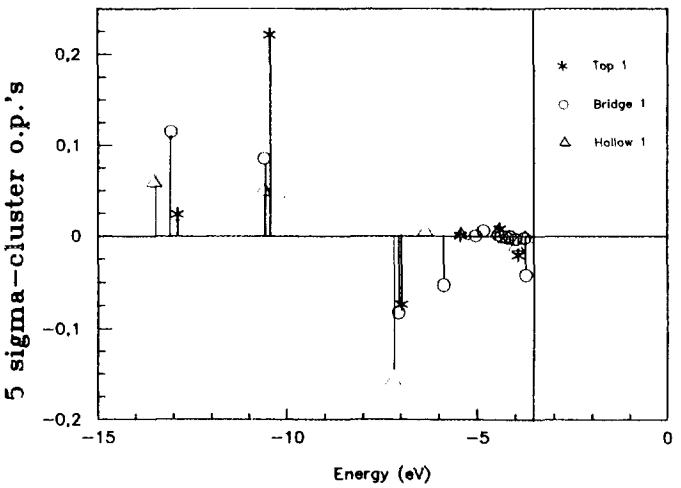

FIG. 4. The cluster orbital overlap population plots of the CO 5σ–cluster interactions of t1 (stars), b1 (circles), and h2 (triangles) levels. Each computed cluster state is given a weight proportional to its contribution to the overlap population between the CO 5σ fragment orbital and all of the bare cluster states. Contributions which strengthen the adsorption bond are positive, weakening contributions are negative.

energy in the case of atop than bridging, and bridging in turn slightly higher than hollow. The rationale for this behaviour, as well as the reason for the unexpected 5σ CO-cluster o.p. behaviour, can be best understood in terms of the group orbitals of the various sites.

Group orbitals are the linear combinations of the pure, unmixed atomic orbitals on a group of atoms. For the atop site, the group of atoms is simply one atom, namely the coordinated Co atom; for the bridging site the group is a cobalt dimer, and for the hollow site it is a Co_3 triangular unit. We have shown previously (21) that by using a group orbital analysis technique, the surface orbitals showed by symmetry to interact with adsorbate orbitals can be "presorted"; thus the resultant PDOS curves will not be diluted by less relevant orbitals.

In the case of interaction with CO 5σ, the group orbital must always be bonding between the metals of the group. We restrict ourselves to a single example, namely the bridging site. Of the group orbitals which are bonding between the Cos, the best overlap with CO 5σ is achieved by the xz a^1 combination. The integration curve of these states is compared to the noninteracting xz a^2 combinations in Fig. 5; the former are indeed pulled down into the peaks formally attributed to CO 4σ and 5σ states. At the atop site, by symmetry, exclusively the z^2 states of Co(1) can interact with the CO 5σ. At the hollow site, the group orbitals must be binding between 3 cobalt centers, thus primarily xz, yz linear combinations of a^1 symmetry. The xz, yz e states, in contrast, cannot interact.

As shown in the schematic diagram in Fig. 6, the more atoms in the binding group, the lower the energy of the states that fulfill the requirements. When the CO 5σ–Co

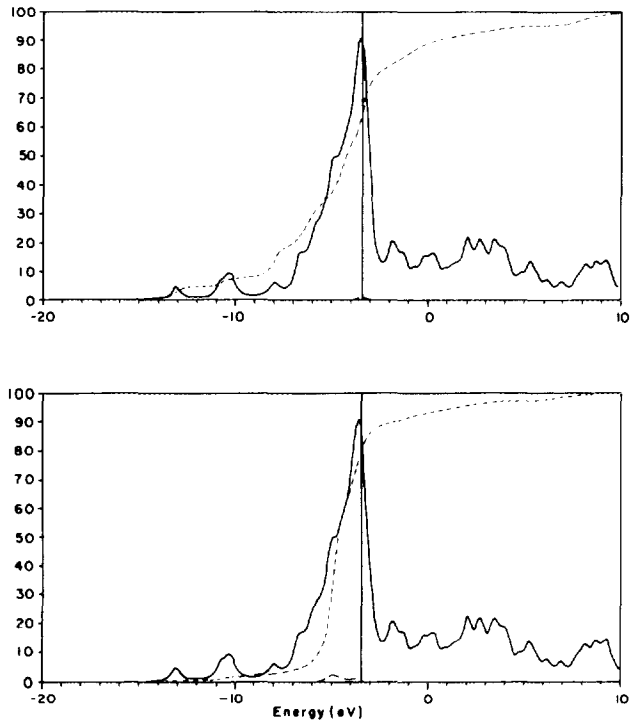

FIG. 5. Example of group orbital analysis: b1. The integration curve of the xz a^1 Co group orbitals is shown in the top panel, along with the total DOS. Note that the group orbital density is significantly pulled down into the formally CO 4σ and 5σ peaks. The integration of the noninteracting xz a^2 combinations are shown in the lower panel.

interaction is "turned on," one finds that the higher the energy of the group orbitals, the higher in energy the resultant CO–cluster antibonding levels will be. Thus we may expect that many of the 5σ–cluster antibonding states are pushed above ε_f for atop sites, resulting in a net positive 5σ–cluster o.p., less for bridging, resulting in approximately zero o.p., and even less for hollow sites, producing a net negative o.p.

The C–O bond can be analyzed in the same way; the C–O o.p. can be split into the 5σ and $2\pi^*$ contributions, as shown in Fig. 7. The total C–O o.p. is also shown. As with the CO–cluster o.p. analysis, the total and component C–O o.p. are dependent primarily on adsorption site, and much less so on cluster size. In this case, the lack of variation in the extent of the 5σ filling is mirrored in its rather uniform contribution to the C–O bond strength. The slight C–O binding character can be noted in the free CO 5σ contribution. The $2\pi^*$ also behaves as expected; the greater the filling, the weaker the C–O bond. The net result is that the greatest bond weakening is observed in the hollow site, and the effect decreases as the coordination number decreases. This is in complete agreement with numerous experimental studies of CO on various transition metal surfaces. The higher the CO coordination, the weaker the C–O bond, as deduced from the downward shift of the CO HREELS frequency, and the increasing chance of CO dissociation.

The dependence on cluster size and the effect of CO adsorption on metal–metal bonds within the clusters can be analyzed by comparing the Co–Co o.p.s. Some influence on the clusters themselves is expected, as it has been shown experimentally that adsorption of certain species can depend on the size of metal clusters (H_2 and H_2O on iron clusters, for example) (22). Table 6 lists the o.p.s between two different types of Co–Co bonds, before and after CO chemisorption. In the case of atop CO geometries, type 1 is between the coordinated Co-atom and its nearest neighbour, and type 2 is between the nearest neighbour and next-nearest neighbour. In the case of bridging or hollow CO coordination geometries, type 1 is

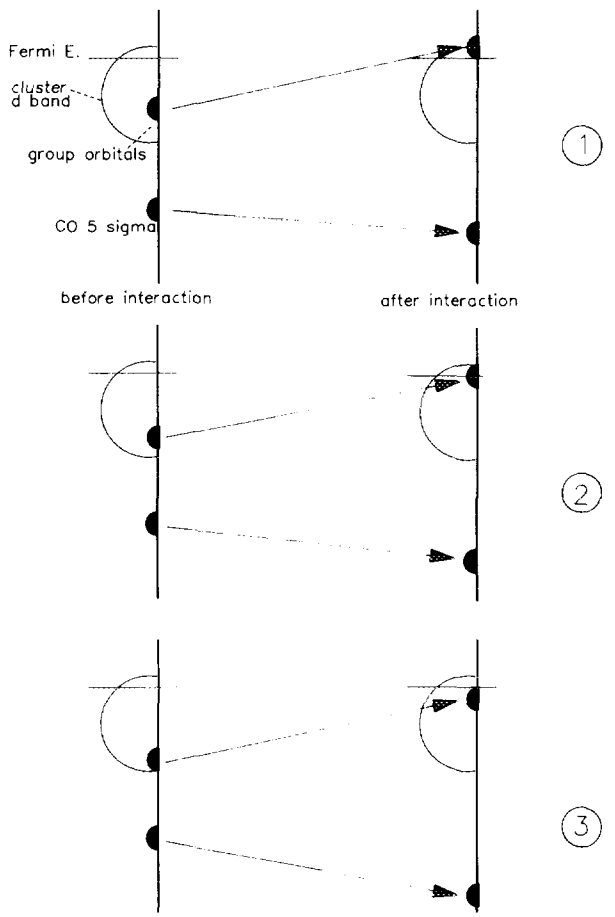

FIG. 6. A schematic interpretation of the 5σ–cluster interactions accentuating the different energy ranges of the relevant cluster group orbitals. In the case of atop coordination (1), the proper group orbitals lie relatively high in energy; thus the resulting 5σ antibonding levels are pushed above ε_f, and the 5σ–cluster o.p. is positive. For bridging geometries (2), the metal levels lie lower, and the resulting 5σ antibonding levels are pushed only partially above ε_f, resulting in a zero o.p. contribution. For hollow geometries (3), the metal level lie even lower, the resulting 5σ antibonding levels remain under ε_f, and the net o.p. is negative.

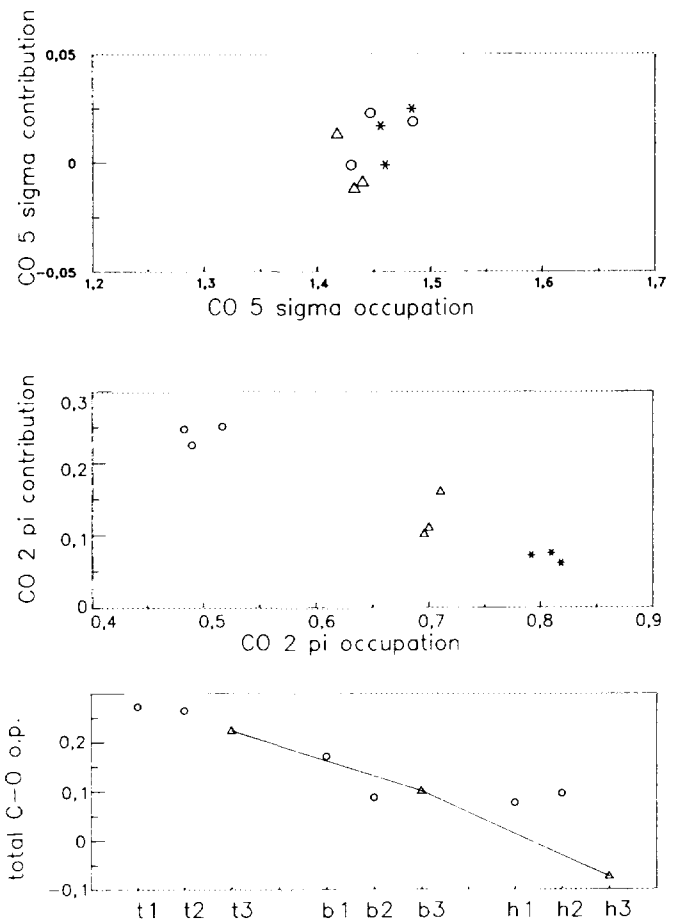

FIG. 7. Decomposition of the C–O overlap population. The top panel shows the contribution to this o.p. from the CO 5σ levels vs the CO 5σ electronic occupation, and the middle panel the same for the CO $2\pi^*$ level. Circles represent atop models, triangles bridging models, and stars hollow models. Note that the electronic occupation scales are equivalent. The bottom panel shows the total C–O o.p. for each model; the 13-atom models are highlighted.

between two Co-atoms directly bonded to CO, and type 2 is between one CO-coordinated metal atom and its nearest neighbour.

CO adsorption consistently reduces the strength of the type 1 surface bonds drastically. The most clear correlation is with cluster size; the larger the cluster, the greater the weakening, in general. The reduction is extreme in some cases. In fact, the metal–metal interaction in b2 even becomes repulsive. A relationship between CO site and the extent of weakening is seen most clearly for the 13-atom clusters; the higher the coordination number of the CO, the weaker the type 1 surface bond. Thus hollow-bound CO weakens this surface bond most strongly. In the weakening of this metal–metal interaction, the importance of the coordination number of the cluster atoms is again clearly illustrated. The extent to which CO adsorption can weaken the type 1 surface bond depends not only on the coordination number of Co(1), but also on the coordination numbers of its nearest neighbours. If the nearest neighbour metal atoms are severely undercoordinated, the influence of CO is not sufficient to overcome the "overbinding" between the metal atoms. For example, the results of the series t1, t2, t3 can be explained by considering that the nearest neighbour Co(2) in t1 has only three neighbours, whereas Co(2) in t2 has four, and Co(2) in t3 has five. Therefore the type 1 bond in t1 is the least affected by CO coordination.

The type 2 surface bond, being somewhat further removed from the adsorption site, is less affected in every case. Bond strength reduction is less than 10% for the traditionally built clusters. For t2, the bond is in fact strengthened slightly. Coordination to the 13-atom clusters induces bond weakening of about 13%. Less variation is observed between the different types of clusters and different CO binding geometries. That the results of the 3 coordination modes to the 13-atom cluster have nearly an identical effect on the type 2 metal–metal bond supports the argument that the coordination numbers of all of the atoms in the cluster are important.

We have only tabulated the effect of adsorption on two of the many metal–metal bonds in the clusters. Comparing the average Co–Co o.p.s before and after CO binding reveals that the CO molecule, in fact, weakens the cluster as a whole. This is important in understanding the variation in the CO–cluster binding energy. The changes observed in the C–O bond as a function of adsorption site are small in comparison to the apparent destructive influence of CO on the cluster. Thus the computed binding

TABLE 6

Co–Co o.ps of Bare Clusters, upon CO Adsorption and Difference as Percentage Reduction

Model	Bare	With CO	% diff.	Bare	With CO	% diff.
		Co(1)–Co(2)			Co(2)–Co(3)	
t1	0.156	0.139	−11.0	0.232	0.214	−7.8
t2	0.104	0.071	−31.7	0.168	0.178	+6.0
t3	0.130	0.055	−57.7	0.130	0.113	−12.8
		Co(1)–Co(1)			Co(1)–Co(2)	
b1	0.124	0.056	−54.9	0.223	0.210	−5.8
b2	0.074	−0.106	−243	0.160	0.147	−8.1
b3	0.130	0.049	−62.3	0.130	0.111	−14.6
		Co(1)–Co(1)			Co(1)–Co(2)	
h1	0.114	0.048	−48.0	0.242	0.221	−8.7
h2	0.110	0.048	−56.8	0.197	0.180	−8.6
h3	0.130	0.014	−89.1	0.130	0.115	−11.7

Note. For atop, Co(1)–Co(2) and Co(2)–Co(3) are listed. For bridging and hollow Co(1)–Co(1), i.e., both metal atoms coordinated to CO, and Co(1)–Co(2), i.e., one metal atom coordinated to CO and one nearest neighbor.

energies will be dominated by terms resulting from electronic changes **within** the metal clusters, i.e., secondary effects of the actual adsorption process. These electronic changes within the cluster will naturally depend primarily on the cluster shape. This may be the central reason for the apparent success of clusters like the 13-atom cluster in computing the relative binding energies of CO properly.

IV. CONCLUSIONS

When clusters are used to model the chemical reactivity of metal surfaces, the coordination numbers of the atoms constituting the clusters must be carefully taken into account. Clusters in which the surfacelike atoms have lower coordination number than the bulklike atoms appear to give more consistent results with regard to the binding energy of adsorbates. The binding energy to clusters which are instead built by taking several surface atoms and adding second layer atoms will be determined largely by the resultant coordination numbers of the model atoms. A second advantage of the 13-atom cluster used in this study is that a variety of adsorption sites can be compared on the same cluster. Thus, for any coordination geometry of the adsorbate, the cluster geometry remains invariant. Thirdly, the coordination number of the model surface atom is constant, independent again of the adsorbate site. The coordination number of a surface atom is very influential in its chemical reactivity; thus, the reactivity of different sites can be compared in an unbiased manner.

Variation in the binding energy of a series of different clusters to the same adsorbate is dominated by effects within the clusters themselves. The clusters are greatly stressed by adsorption, as seen by the large decrease in the intermetallic bond strengths (overlap populations). The extent to which adsorption can reduce metal–metal bonding is largely determined by the coordination numbers of the metal atoms and their nearest neighbours. Although the metal–adsorbate bond strength, as well as internal adsorbate bond strengths, varies with adsorption site, the range is much less than the reduction in metal–metal bond strength.

The overlap population analysis also reveals that the "chemical reactivity" is quite site-sensitive, and thus adequately modeled by either type of cluster. Very important is the fact that cluster size is much less influential in these parameters than it is in energetic considerations. Second, site preference, C–O HREELS frequency, and dissociation probabilities can be modeled correctly on a relative scale.

A detailed understanding of the electronic structure of adsorbate–adsorbent systems is in our minds the key to understanding the experimental data on surface reactions. This knowledge can be used to predict the catalytic behaviour of metal surfaces, and to study the elementary steps in catalytic reactions such as Fischer–Tropsch synthesis.

REFERENCES

1. Blyholder, G., *J. Phys. Chem.* **68,** 2772 (1964).
2. see, for example, Albright, T. A., *Tetrahedron Rep.* **126,** 1339 (1981).
3. Geerlings, J. J. C., Zonnevylle, M. C., and de Groot, C. P. M., *Catal. Lett.* **5,** 309 (1990); Geerlings, J. J. C., Zonnevylle, M. C., and de Groot, C. P. M., *Surf. Sci.* **241,** 302, 315 (1991).
4. Koutecky, J., and Fantucci, P., *Chem. Rev.* **86,** 539 (1986).
5. Baerends, E. J., Ellis, D. E., and Ros, P., *Chem. Phys.* **2,** 41 (1973); Baerends, E. J., and Ros, P., *Chem. Phys.* **2,** 52 (1973); Baerends, E. J., and Ros, P., *Chem. Phys.* **8,** 412 (1975).
6. see, for example, van den Hoek, P. J., Baerends, E. J., and van Santen, R. A., *J. Phys. Chem.* **93,** 6469 (1989); Jansen, A. P. J., and van Santen, R. A., *J. Phys. Chem.* **94,** 6764 (1990); Ellis, D. E., Guo, J., and Cheng, H. P., *J. Phys. Chem.* **92,** 3024 (1988).
7. Ziegler, T., and Rauk, A., *Theor. Chim. Acta* **46,** 1 (1977).
8. Snijders, J. G., Vernooijs, P., and Baerends, E. J., *At. Data Nucl. Data Tables* **26,** 143 (1981); Internal Report, Free University, Amsterdam, 1981, unpublished.
9. Zonnevylle, M. C., Geerlings, J. J. C., and van Santen, R. A., *Surf. Sci.* **240,** 253 (1990).
10. Kittel, C., "Introduction to Solid Sate Physics," Wiley, New York, 1976.
11. Bagus, P. S., Nelin, C. J., and Bauschlicher, C. W., *Phys. Rev. B.* **28,** 5423 (1983).
12. Post, D., and Baerends, E. J., *Surf. Sci.* **116,** 177 (1982); Post, D., and Baerends, E. J., *J. Chem. Phys.* **78,** 5663 (1983).
13. see also Hoffmann, R., "Solids and Surfaces. A Chemist's View of Bonding in Extended Structures," VCH, New York, 1989.
14. Fauster, Th., and Himpsel, F. J., *Phys. Rev. B* **27,** 1390 (1983).
15. Demuth, J. E., Schmeisser, D., and Avouris, Ph., *Phys. Rev. Lett.* **47,** 1166 (1981).
16. Backx, C., and de Groot, C. P. M., unpublished results.
17. Papp, H., *in* "Proceedings, IVC-8, ICSS-4, ECOSS-3, Cannes, 1980," p. 245; Papp, H., *Surf. Sci.* **129,** 205 (1983).
18. van Santen, R. A., *Prog. Surf. Sci.* **25,** 253 (1987); *J. Mol. Struct.* **173,** 157 (1988); *J. Chem. Soc., Faraday Trans.* **83,** 1915 (1987).
19. see, for example, Ishi, S., Ohno, Y., and Viswanathan, B., *Surf. Sci.* **161,** 349 (1985).
20. Hughbanks, T., and Hoffmann, R., *J. Am. Chem. Soc.* **105,** 1150 (1983); Wijeyesekera, S. D., and Hoffmann, R., *Organometallics* **3,** 949 (1984).
21. Zonnevylle, M. C., Hoffmann, R., van den Hoek, P. J., and van Santen, R. A., *Surf. Sci.* **223,** 233 (1989).
22. Weiller, B. H., Bechthold, P. S., Parks, E. K., Pobo, L. G., and Riley, S. T., *J. Chem. Phys.* **92,** 8618 (1992).